Differential cross-section measurements of multiply charged xenon ions produced in 10–28-keV e^--Xe collisions

S. Mondal and R. Shanker*
Atomic Physics Laboratory, Department of Physics, Banaras Hindu University, Varanasi 221 005, India
(Received 2 August 2005; published 8 November 2005)

Partial single-differential ionization cross sections (PSDICSs) of a multiply ionized xenon atom (Xe^{n+}, $n=1-7$) are measured for impact of 10–28 keV electrons with xenon by performing coincidences between the produced recoil ions and the electrons of indiscriminated energies detected at 90° with respect to the incident electron beam direction. Values of relative PSDICSs for doubly charged ions are found to be about 25% larger than those for singly charged ions in the considered impact energy range. The examination of charge-state fractions and relative cross-section fractions of multiply charged ions as a function of incident electron energy suggests that the multiply charged ions are produced via creation of an inner-shell vacancy followed by Auger and shakeoff processes. The mean charge state of the ions produced in the collisions is found to be independent of the impact energy and reaches a constant value close to 2.6. The Fano-Bethe plots of the PSDICSs suggest that higher charge states of the ions are weakly produced via optical transitions; moreover, the latter process becomes a dominant channel for producing the doubly charged ions that are correlated with the electrons detected at 90°.

DOI: 10.1103/PhysRevA.72.052705 PACS number(s): 34.50.Fa, 34.80.Dp

I. INTRODUCTION

In multielectron ionizing collisions involving an energetic charged particle and a many-electron atomic target, the lowest order of ionization process involves generally a single interaction between the projectile and the target electron. However, in the multiple ionization of the target, a substantial probability of ionization occurs due to the multiple interactions between the projectile and the target electrons as well as among the target electrons themselves. The former type of interaction leading to single ionization can be explained reasonably well by the Born approximation method. However, a detailed understanding of the multiple-ionization processes is far from a complete picture. This situation has naturally resulted in the motivation for several recent studies of multiple ionization of many-electron atoms under charged-particle [1–6] and photon impact [7,8]. Andersen *et al.* [9] have measured single- and multiple-ionization cross sections of several atomic targets by fast protons and antiprotons with impact energy ranging from 0.5 to 5 MeV. For a He atom, they observed that the single-ionization cross sections are the same for all singly charged projectiles of equal velocity, while the double-ionization cross sections for impact of antiprotons and electrons are larger by as much as a factor of 2 than those obtained for impact of protons. Interest in exploring the cause of this difference has motivated extensive theoretical calculations incorporating different mechanisms. McGuire [10] has suggested that this difference may be present due to the interference effect stemming from different collision mechanisms. Recently, McGuire [11] has offered a rigorous discussion of shakeoff and two-step processes and has shown them to be responsible for the above difference. However, for a many-electron atom, the inner-shell ionization followed by Auger and Coster-Kronig transitions and subsequent rearrangement of inner-shell holes leads to the multiple ionization of the target atom. Our recent measurements [12] on partial double-differential ionization cross sections (PDDICSs) of argon have suggested that the singly charged ions are mainly produced due to direct outer-shell ionization, while multiply charged ions are produced mainly due to Auger and shakeoff processes. Xenon being a multielectron system has provided a suitable test ground to elucidate such many-electron problems and it has motivated several workers to study multiple ionization in the recent past [13–19]. However, most of the experimental works on xenon have concentrated on the measurements of total ionization cross sections, which obviously do not provide a detailed insight into the mechanism of multiple-ionization processes of the atom. The only PDDICSs measurements of xenon to our knowledge have been made by Chaudhry *et al.* [20] for incident electrons of energies between 1 and 8 keV. They suggested that vacancy creation in the inner shell, such as the L shell can result in more higher-charge states of the atom than vacancy creation in its outer M or N shell. Theoretically also, studies of multiple ionization of xenon have concentrated on calculations for the total ionization cross sections. Recently, Bartlett and Stelbovics [21] measured the total ionization cross sections of xenon by impact of electrons having energy from threshold to 3 keV and compared their data with Born calculations using high-quality Hartree-Fock Slater orbitals.

In the present work, the partial single-differential ionization cross sections (PSDICSs) of xenon ions produced in 10–28-keV e^--Xe collisions have been measured by performing coincidences between the multiply charged xenon ions and the electrons of indiscriminated energies that are detected at 90° with respect to the incident beam direction. These measurements are undertaken for twofold reasons: first, because no multiple-ionization PSDICS or PDDICS

*Electronic address: rshanker@bhu.ac.in

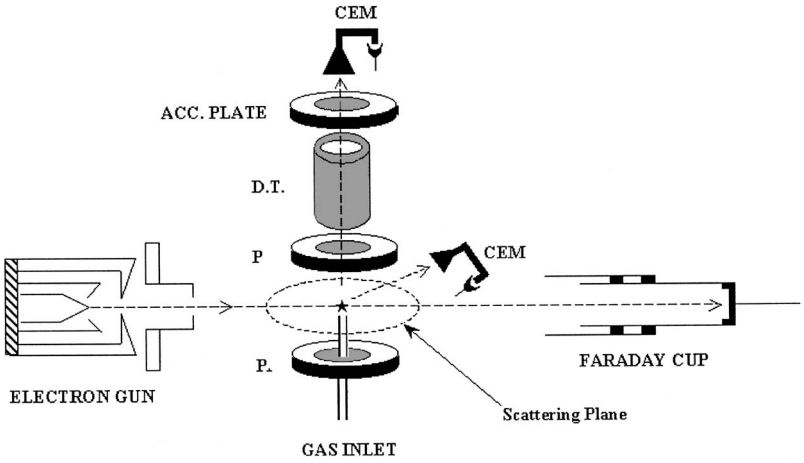

FIG. 1. Schematic diagram of the experimental setup.

studies of xenon have been reported earlier for this range of electron impact energies, to our knowledge; and second, in this impact energy region, the dominant role in producing the multiple ionization of atoms is known to be played by a two-step process [22]. Also, the present data are expected to provide further insight into the collision mechanism for producing multiply charged ions of the target atom compared to those obtained from a simple mass spectrometric determination of different charged-state ions [13–16].

II. EXPERIMENTAL TECHNIQUE

The PSDICSs of xenon were measured by using a slow electron–recoil ion coincidence technique in an experimental facility that has been described in detail previously elsewhere [12,23]. In brief, the setup is essentially a crossed-beam-type facility in which a monoenergetic electron beam of 3 mm diameter cross fires a well-collimated beam of target atomic gas effusing from a hypodermic needle ($\Phi \sim 1$ mm) (see Fig. 1). After transmitting through the gaseous target, the incident electron beam was made to strike a biased (−60 V) Faraday cup. The secondary electrons (primary scattered+ejected) of indiscriminated energy were detected at 90° with respect to the incident electron beam direction and were monitored by a channel electron multiplier (CEM) operating in a pulse-counting mode with a narrow solid angle ($d\Omega_e = 0.03$ sr). The reduction of earth's magnetic field near the collision zone was necessary to minimize the deflection of low-energy electrons reaching the detector. This was accomplished by using a 0.5-mm-thick antimagnetic μ-metallic shielding inside the wall of reaction chamber. The multiply charged ions produced in the interaction region were extracted and charge analyzed by a time-of-flight (TOF) spectrometer [24]. The ions were extracted by an electric field of 260 V/cm. The applied electric field was set perpendicular to the direction of detected electrons entering the channeltron as well as to the direction of incident electrons. The extraction field was produced by applying equal and opposite potentials to two horizontally mounted parallel plates (18 mm apart) enclosing the collision zone. The tip of the gas jet was positioned in the middle of the two plates and pierced vertically into the lower plate from underneath. Under this configuration, the electrons viewed by the channeltron were not affected by the presence of the extraction field. This was confirmed by observation that no noticeable change took place in shape and measured counts of the detected electrons with and without the applied extraction field. The extraction field was optimized for a full extraction of Xe^+ ions (slowest ions) and for their full transmission in the time-of-flight spectrometer. After extracting the ions, they were further accelerated into the drift tube biased at −365 V and were made to travel in a field-free region of about 22 mm path length. At the end of the drift tube, the ions were post-accelerated by applying a field of −1100 V and were finally detected by a channeltron biased at +3.5 kV. To investigate the PSDICSs for multiple ionization of xenon using the coincidence technique, it was necessary to ensure an accurate alignment of the electron beam, the TOF spectrometer, and the electron detector with respect to the collision center. The TOF spectrum of ions was obtained as a function of the time delay between the TOF of recoil ions of different charge states and the corresponding electrons of all energies detected at an angle $\theta_\delta = 90°$ with respect to the incident electron beam direction. The PSDICSs of xenon ions were measured by detecting coincidences between the electrons detected at angle $\theta_\delta = 90°$ to the incident beam direction and the simultaneously produced recoil ions. From the detected true total coincidence count N^{n+} of the n-fold-ionized atoms, the experimental relative PSDICSs, $d\sigma_{ni}/d\Omega_e$ were obtained by using the relation

$$\sigma_{ni}(\theta_\delta) = \frac{d\sigma_{ni}}{d\Omega_e} = \frac{1}{\varepsilon^{n+}} \frac{N^{n+}}{N_0 P L} \frac{1}{d\Omega_e} \frac{1}{3.34 \times 10^{16}} \text{ cm}^2 \text{ Sr}^{-1} \tag{1}$$

where N_0 is the measured total number of incident beam particles, P is the pressure of the target gas in Torr, L is the effective path length of the collision region in cm, $d\Omega_e$ is the solid angle subtended by the channeltron on the collision center in sr, and ε^{n+} is the detection efficiency of the CEM for detecting ions of charge state $n+$. The uncertainty involved in measurements of the relative PSDICS of xenon ions is estimated to be about 30%.

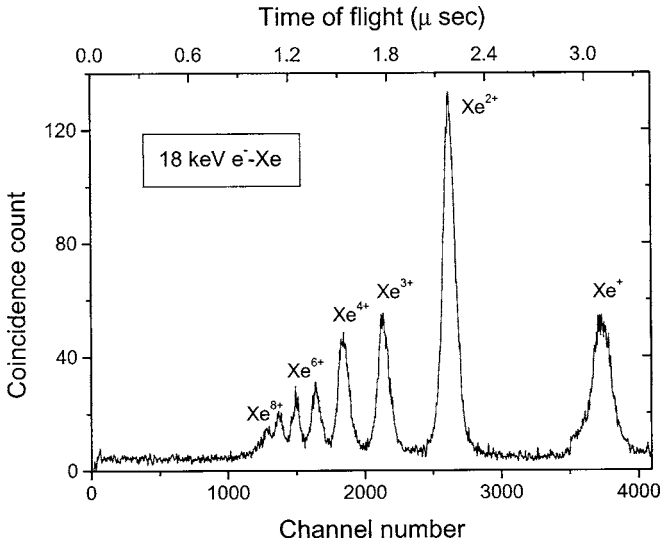

FIG. 2. Time-of-flight spectrum of multiply charged xenon ions observed in coincidence with secondary electrons of indiscriminated energies detected at 90° with respect to the incident beam direction for 18-keV electron impact with xenon.

III. RESULTS AND DISCUSSION

A typical time-of-flight spectrum of the multiply charged xenon ions produced from collisions of 18-keV electrons with xenon is displayed in Fig. 2. It is seen that the Xe^{n+} ions are produced with charge states as high as $n=8$. It is also noted that the relative intensity of doubly charged ions is considerably larger than that of singly as well as of all other highly charged ions. Similar behavior is observed for ions produced in collisions of electrons of other impact energies with xenon atom. This feature is reflected from Fig. 3 which shows the variation of relative PSDICSs of multiply charged xenon ions produced in the considered collisions as a function of incident electron energy. Generally, the singly charged ions are produced due to direct ionization of the target atom by incident charged particles ejecting a large

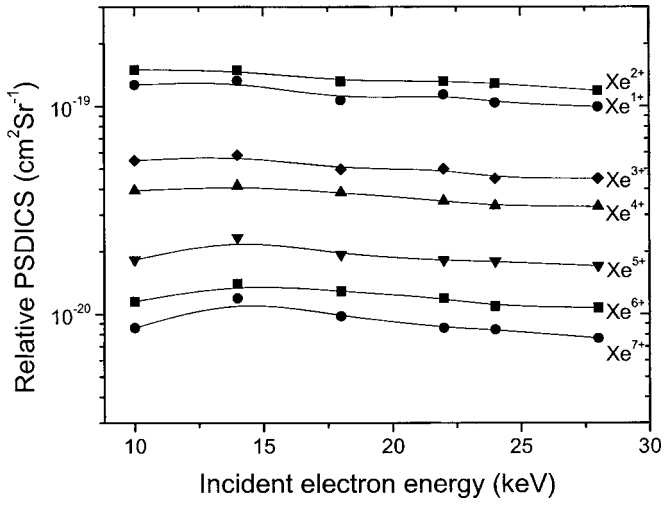

FIG. 3. Partial single-differential n-fold ionization cross sections of xenon ($n=1-7$) as a function of the incident electron energy.

number of secondary electrons of low energies in the forward direction with respect to the incident electrons following binary encounter events [25]. Hence, in the multiple ionization of an atom by impact of a charged particle, the singly charged ions are observed in larger intensity than the multiply charged ions when they are detected without considering the correlated electrons detected at an angle. Such type of ion intensity variation has been observed in the study of electron-induced multiple ionization of xenon by Schram [14], El-Sherbini *et al.* [15], and Almeida *et al.* [17]. In contrast, our coincidence results show that the singly charged xenon ions are produced lower in intensity than the doubly charged xenon ions (see Figs. 2 and 3). This difference in ion intensities can be explained as follows. The secondary electrons that are produced in multiple-ionization events are believed to originate via two-step processes, such as Auger and Coster-Kronig transitions and shakeoff. In the present study of multiple ionization of xenon, the doubly charged ions are found to originate mainly from N_{45}-O_1O_{23} Auger transitions. The electrons ejected from the O_1 subshell in the Auger process follow an isotropic angular distribution. This angular distribution is not similar to what is shown by electrons emitted in the binary-encounter interaction producing singly charged xenon ions. Consequently, the number of electrons ejected at 90° by a direct ionization process and correlating with the singly charged ions is much less than the number of electrons ejected at 90° by the two-step process yielding doubly charged ions. The above explanation is also supported by the results of Chaudhry *et al.* [20] who have shown that the PDDICSs of doubly charged xenon ions dominate the PDDICSs of the singly charged ions when they are detected in coincidence with the secondary electrons ejected at 90° for a wide range of their energies. They have further found that due to the N_{45}-O_1O_{23} Auger transitions involving secondary electrons of 32.8 eV, the PDDICSs for double ionization are larger than those for single ionization. Also, for secondary electrons of higher energies, the PDDICS value of double ionization dominates over the PDDICS value for single ionization due to several additional single [26] and double [27] Auger transitions for incident electron energies above 6.0 keV [20].

The time-of-flight spectra allow us to determine the mean charge state $\bar{n}$ of the multiply charged xenon ions observed in coincidence with the secondary electrons detected at 90°. The $\bar{n}$ can be calculated using the relation

$$\bar{n} = \sum_n (N^{n+} n) \Big/ \sum_n N^{n+}. \tag{2}$$

Figure 4 shows the variation of mean charge state $\bar{n}$ as a function of the incident energy. It suggests that the mean charge state obtains almost a constant value of $\bar{n}=2.6$ and that it is independent of the impact energy. The calculated error on the mean charge state is about 2% which is within the size of the data symbols shown in the figure.

In order to investigate the possible mechanisms involved in multiple ionization of xenon atoms, we have determined the charge-state fractions F_n ($F_n=N^{n+}/\Sigma_n N^{n+}$, where the sum is extended in the denominator up to the highest observed charged state n) of the multiply charged ions and have ex-

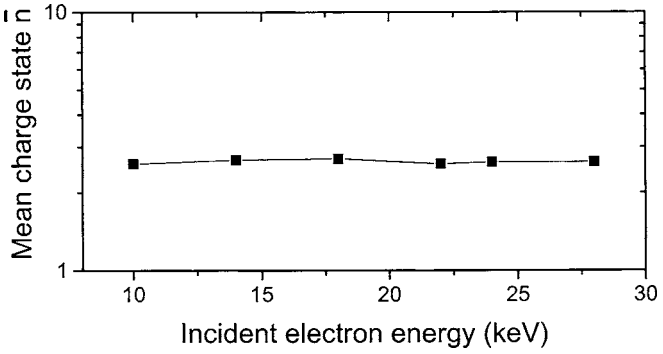

FIG. 4. Mean charge state $\bar{n}=(\Sigma N^{+}n/\Sigma_n N^{+})$ as a function of incident electron energy. Solid line is shown to guide the eyes through the data points.

amined their variations as a function of incident electron energy. This variation is shown in Fig. 5. The maximum error in measurements of the charge-state fractions is about 3% and the margin of fitting errors is found to vary in the range 2–5 %; corresponding error bars for each data point remain within the symbol size. However, the scatter in data points at 18 keV may be due to an unknown experimental problem. It is seen that the F_n values for singly charged ions decrease with incident energy whereas their values for multiply charged ions obtain almost a constant value for the considered incident energies. The reason for the former observation is that due to the binary-encounter process, the directly ionized electrons correlated with the singly charged ions are ejected increasingly more in the forward direction with increasing incident energy. Hence, the probability for emission of directly ejected electrons at 90° with simultaneous production of singly charged ions decreases with increasing incident energy. However, in the case of the latter observation, the produced ions arise from inner-shell ionization followed by Auger and shakeoff processes. Further, the secondary electrons which are generated by a shakeoff process are produced due to inner-shell rearrangement; this rearrangement of electrons is known to be independent of the charge and the

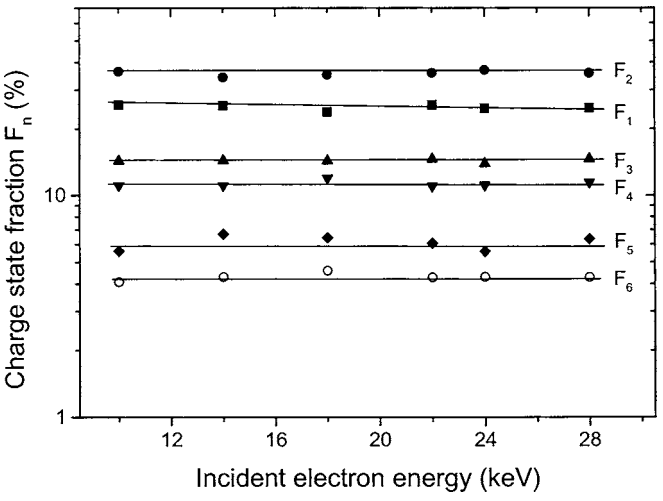

FIG. 5. Charge-state fractions $F_n=(N^{n+}/\Sigma_n N^{n+})$ as a function of impact energy.

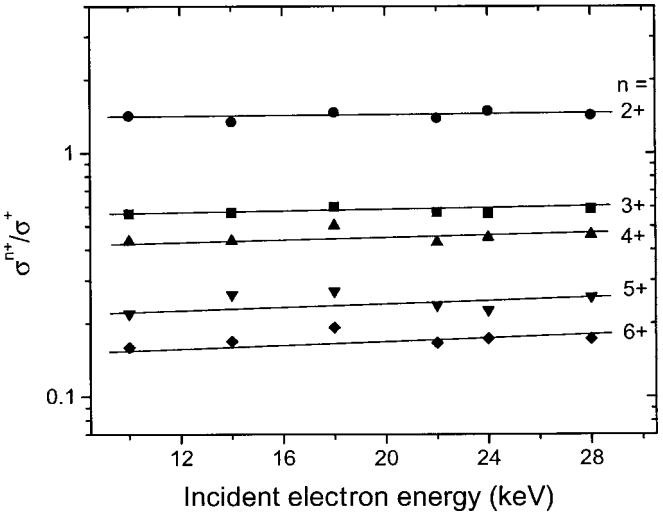

FIG. 6. Relative cross-section fractions $R_n=(\sigma^{n+}/\sigma^{+})$ of different charge states n as a function of impact energy.

velocity of the incident projectile [12,22]. Therefore, the charge-state fractions for multiply charged ions attain a constant value in the region of impact energy considered here.

To shed further light into the mechanisms involved in multiple ionization of xenon, we have obtained the relative PSDICS fractions ($R_n=\sigma^{n+}/\sigma^{+}$) of multiply charged xenon ions Xe^{n+} ($n=2-6$) with respect to the singly charged ions. These are plotted as a function of incident energy for the range of 10–28 keV and are shown in Fig. 6. The maximum error involved in determination of the R_n is about 3%, which is within the size of the data symbols. It is seen from the figure that the R_n values for different charge states increase with impact energy. This behavior arises because as the incident energy increases, the PSDICS for a singly charged ion decreases (see Figs. 3 and 5), whereas the PSDICS for higher (multiply) charged ions remains almost constant. Further, Fig. 6 shows that as the charge state of the ions increases, the relative slope of the corresponding curves increases. This behavior occurs because the decreasing effect of the PSDICS reduces with increasing incident energy as the charge state attains a higher value (see Fig. 3).

To obtain more information on the ionization mechanism in the considered collision system, the PSDICS values of the produced xenon ions have been compared with theoretical calculations based on the Born approximation. For high velocity of incident electrons, the n-fold ionization cross sections of the target atom can be written using the Bethe formula [15]

$$\sigma_{ni}(\theta_\delta)=\frac{4\pi a_0^2 R}{E_{\mathrm{el}}}M_{ni}^2 \ln c_{ni}E_{\mathrm{el}} \tag{3}$$

where $\sigma_{ni}(\theta_\delta)$ is the angular differential ionization cross section for formation of $n+$ ions in $\mathrm{cm}^2\,\mathrm{sr}^{-1}/\mathrm{atom}$, E_{el} is the incident electron energy, a_0 is the first Bohr radius, R is the Rydberg energy, and c_{ni} is a constant. M_{ni}^2 is equal to the square of the dipole matrix element divided by a_0^2. For n-fold ionization of an atom, M_{ni}^2 is related to the differential optical oscillator strength f as

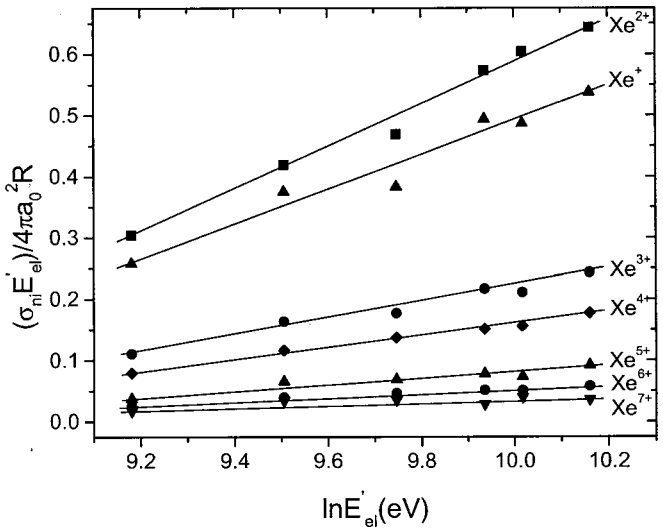

FIG. 7. Fano-Bethe plots: $\sigma_{ni}E'_{\mathrm{el}}/4\pi a_0^2 R$ versus $\ln E'_{\mathrm{el}}$ for Xe^{n+} ions produced in 10–28-keV e^--Xe collisions.

$$M_{ni}^2 = \int_{V_{\mathrm{ion}}}^{\infty} \frac{df}{dE}\frac{R}{E}dE. \tag{4}$$

Here the integration is taken over the continuum, E is the energy of the continuum electrons, and V_{ion} is the ionization potential.

For the present impact energies, it is necessary to correct them for relativistic effect. Hence using the relativistic incident electron energy E'_{el}, Eq. (3) can be written as

$$\frac{\sigma_{ni}(\theta_\delta)E'_{\mathrm{el}}}{4\pi a_0^2 R} = M_{ni}^2 \ln E'_{\mathrm{el}} + C_{ni} \tag{5}$$

where C_{ni} is another constant equal to $M_{ni}^2 \ln c_{ni}$. Now, by plotting the experimental $\sigma_{ni}(\theta_\delta)E'_{\mathrm{el}}/4\pi a_0^2 R$ values as a function of $\ln E'_{\mathrm{el}}$ for different charge states n, one obtains a curve whose gradient gives the value of M_{ni}^2. These values provide information on the dipole oscillator strength for production of different ionic charge states and hence on the strength of the corresponding optical transitions.

Figure 7 shows the Fano-Bethe plots for the variation of $\sigma_{ni}(\theta_\delta)E'_{\mathrm{el}}/4\pi a_0^2 R$ versus $\ln E'_{\mathrm{el}}$ for different charge states $n=1-7$ of xenon ions. The M_{ni}^2 values for Xe^{n+} ions are listed in Table I. From this table, it is noted that the value of M_{ni}^2 decreases with increasing charge state in going from $n=1$ to 7; however, for doubly charged ions, M_{ni}^2 obtains the largest value compared to ions of other charge states. The decrease of M_{ni}^2 values with charge state suggests that the probability for production of higher-charge-state ions through optically allowed transitions decreases with increasing charge state of ions. Nonetheless, the M_{ni}^2 value for doubly charged xenon ions is found to be about 25% larger than that for singly charged ions, which in turn suggests that the electrons detected at 90° by optically allowed transitions with simultaneous production of Xe^{2+} are larger than that for producing Xe^+. This situation occurs due to a very small fraction of directly ejected electrons at 90° with simultaneous production of singly charged ions. In contrast, it is seen that the doubly charged xenon ions are mostly produced via N_{45}-O_1O_{23} Auger transitions while the production of Xe^{2+} via direct ionization is extremely low. Since the Auger electrons follow an isotropic angular distribution (as discussed earlier), the electrons detected at 90° in coincidence with Xe^{2+} ions would therefore result in larger cross sections for Xe^{2+} ions than that for Xe^+ and hence the larger M_{ni}^2 value for Xe^{2+}.

TABLE I. Comparison of electron impact M_{ni}^2 values derived from the present PSDICS coincidence measurements with those from noncoincident data of other workers.

Ions	Present work	Sherbini *et al.* [15]	Schram *et al.* [14]
Xe^+	$(2.8\pm0.3)\times10^{-1}$	4.50 ± 0.09	5.25
Xe^{2+}	$(3.5\pm0.2)\times10^{-1}$	1.30 ± 0.04	1.45
Xe^{3+}	$(1.2\pm0.1)\times10^{-1}$	$(8.0\pm0.4)\times10^{-1}$	5.5×10^{-1}
Xe^{4+}	$(9.4\pm0.5)\times10^{-2}$	$(3.3\pm0.3)\times10^{-1}$	1.9×10^{-1}
Xe^{5+}	$(4.7\pm0.8)\times10^{-2}$	$(4.5\pm1.2)\times10^{-2}$	
Xe^{6+}	$(3.1\pm0.3)\times10^{-2}$	$(2.9\pm0.6)\times10^{-2}$	
Xe^{7+}	$(1.7\pm0.7)\times10^{-2}$		

The comparison of M_{ni}^2 values obtained in the present work with those of the Schram *et al.* [14] and Sherbini *et al.* [15] shows a larger deviation (about one order of magnitude) for formation of lower-charge states compared to the deviation for formation of higher-charge states (see Table I). This difference is believed to arise due to the fact that in the present measurements, the multiply charged ions are detected in coincidence with the electrons that are detected at 90° whereas Schram *et al.* and Sherbini *et al.* have detected the total multiply charged ions by employing a condenser plate technique without considering what happens to the secondary electrons. Electrons that are ejected at 90° for production of lower-charged states by the direct ionization process have been found to be less in number than in production of higher-charge states. Nonetheless, a reasonably good agreement is observed for M_{ni}^2 values of higher-charge states with those of other workers (see Table I). This happens because the contribution of direct ionization rapidly reduces with increasing charge states of the ions.

IV. SUMMARY

Experimental results on partial single-differential ionization cross sections for multiple ionization of xenon by impact of 10–28-keV electrons are obtained by using coincidences between recoil ions and slow electrons of indiscriminated energies detected at 90° with respect to the incident beam direction. It is observed that the PSDICS of doubly charged xenon ions is larger than that for the singly charged ions as well as for other highly charged ions. This observation suggests that the singly charged xenon ions are mostly produced due to direct ionization of the target; however, the doubly charged ions are produced by an Auger process. The variation of PSDICS for multiply charged ions shows a gradual decrease with increasing electron impact energy. The mean charge state of the multiply charged ions is found to be about

$\bar{n}$=2.6 and to remain constant in the considered incident energy range. The examination of the variation of charge-state fractions and of the relative cross-section fractions of the multiply charged ions with incident electron energy further suggests that the highly charged state ions are predominantly produced by the shakeoff process. Comparison of our measured PSDICSs with the Born approximation calculations shows that the measurement of recoil ions in coincidence with the electrons detected at 90°, the optical oscillator strength for formation of Xe^{2+} is about 25% larger than that for formation of Xe^{+}. The Fano-Bethe plots of multiply charged ions suggest that the production of higher-ionic-charge states via optically allowed transitions decreases with ionic charge state; however, the inner-shell ionization and subsequent shakeoff processes become more dominant channels for producing the higher-charge states of the ions.

ACKNOWLEDGMENTS

The authors acknowledge financial support from Department of Science and Technology (DST), New Delhi for conducting this work under Research Project No. SP/S2/L-08/2001. The authors are also thankful to Professor S. N. Thakur for sparing a channel electron multiplier used in the present experiments. S.M. thanks the DST and the Council of Scientific and Industrial Research (CSIR), New Delhi for providing partial financial support during the execution of this work.

[1] M. T. Huang, W. W. Wong, M. Inokuti, S. H. Southworth, and L. Young, Phys. Rev. Lett. **90**, 163201 (2003).
[2] A. C. F. Santos, A. Hasan, and R. D. Dubois, Phys. Rev. A **69**, 032706 (2003).
[3] A. C. F. Santos, A. Hasan, T. Yates, and R. D. Dubois, Phys. Rev. A **67**, 052708 (2003).
[4] B. Gstir, S. Denifl, G. Hanel, M. Rummele, T. Fiegele, P. Cicman, S. Matejcik, P. Scheier, K. Becker, A. Stamatovic, and T. D. Mark, J. Phys. B **35**, 2993 (2002).
[5] A. Kobayashi, G. Fujiki, A. Okaji, and T. Masnoka, J. Phys. B **35**, 2087 (2002).
[6] M. A. Chaudhry, A. J. Duncan, R. Hippler, and H. Kleinpoppen, Phys. Rev. A **39**, 530 (1989).
[7] H. Wabnitz, A. R. B. de Castro, P. Gurtler, T. Laamann, W. Laasch, J. Schulz, and T. Moller, Phys. Rev. Lett. **94**, 023001 (2005).
[8] J. B. Bluett, D. Lukic, and R. Wehlitz, Phys. Rev. A **69**, 042717 (2004).
[9] L. H. Andersen, P. Hvelplund, H. Knudsen, S. P. Moller, A. H. Sorensen, K. Elsener, K. G. Rensfelt, and E. Uggerhoj, Phys. Rev. A **36**, 3612 (1987).
[10] J. H. McGuire, Phys. Rev. Lett. **49**, 1153 (1982).
[11] J. H. McGuire, *Electron Correlation Dynamics in Atomic Collisions* (Cambridge University Press, Cambridge, U.K., 1997).
[12] S. Mondal and R. Shanker (unpublished).
[13] B. L. Schram, F. J. De Heer, M. J. Van Der Wiel, and J. Kistemaker, Physica (Amsterdam) **31**, 94 (1965).
[14] B. L. Schram, Physica (Amsterdam) **32**, 197 (1966).
[15] T. M. El-Sherbini, M. J. Van Der Wiel, and F. J. De Heer, Physica (Amsterdam) **48**, 157 (1970).
[16] W. Groh, A. Muller, A. S. Schlachter, and E. Salzborn, J. Phys. B **16**, 1997 (1983).
[17] D. P. Almeida, J. Electron Spectrosc. Relat. Phenom. **122**, 1 (2002).
[18] R. Rejoub, B. G. Lindsay, and R. F. Stebbings, Phys. Rev. A **65**, 042713 (2002).
[19] L. Partanen, R. Sankari, S. Osmekhin, Z. F. Hu, E. Kukk, and H. Aksela, J. Phys. B **38**, 1881 (2005).
[20] M. A. Chaudhry, A. J. Duncan, R. Hippler, and H. Kleinpoppen, Phys. Rev. Lett. **59**, 2036 (1987).
[21] P. L. Bartlett and A. T. Stelbovics, Phys. Rev. A **66**, 012707 (2002).
[22] D. Fischer, R. Moshammer, A. Dorn, J. R. C. Lopez-Urrutia, B. Feuerstein, C. Hohr, C. D. Schroter, S. Hagmann, H. Kollmus, R. Mann, B. Bapat, and J. Ullrich, Phys. Rev. Lett. **90**, 243201 (2003).
[23] R. K. Singh, S. Mondal, and R. Shanker, J. Phys. B **36**, 489 (2003).
[24] R. K. Singh, R. K. Mohanta, M. J. Singh, R. Hippler, and R. Shanker, Pramana, J. Phys. **58**, 631 (2002).
[25] S. Mondal and R. Shanker, Phys. Rev. A **69**, 060701(R) (2004).
[26] W. A. Coglan and R. E. Clansing, At. Data **5**, 317 (1969).
[27] W. Mehlhorn, in *Auger-Electron Spectroscopy of Core Levels of Atoms in Atomic Inner-Shell Physics*, edited by B. Craseman (Plenum, New York, 1985), p. 121.